INTERNATIONAL JOURNAL OF ROBUST AND NONLINEAR CONTROL
Int. J. Robust Nonlinear Control (2016)
Published online in Wiley Online Library (wileyonlinelibrary.com). DOI: 10.1002/rnc.3687

Adaptive consensus algorithms for real-time operation of multi-agent systems affected by switching network events

Filiberto Muñoz[1,2], Eduardo Steed Espinoza Quesada[1,5], Hung M. La[3,*,†], Sergio Salazar[2], Sesh Commuri[3,5] and Luis Rodolfo Garcia Carrillo[4]

[1]*Polytechnic University of Pachuca, Hidalgo 43830 Mexico*
[2]*UMI-LAFMIA, DCA, CINVESTAV, Mexico City, 07360 Mexico*
[3]*Computer Science and Engineering, University of Nevada Reno, NV 89557-0171, USA*
[4]*Department of Electrical and Biomedical Engineering, University of Nevada Reno, NV 89557-0260, USA*
[5]*Nevada Advanced Autonomous Systems Innovation Center, University of Nevada Reno, NV 89557-0720, USA*

SUMMARY

We propose a control strategy based on distributed adaptive leader-follower consensus algorithms for multi-agent systems (MAS) affected by switching network events. The strategy allows each agent in the MAS to compute its own control input based on local information and information coming from its neighbors. In this sense, MAS distributed control laws are obtained where the coupling gain of the associated communication graph is adapted dynamically in real-time. The consensus algorithm is extended with a switching network topology approach, which ensures appropriate performance even when the MAS network topology is prone to arbitrary switching. A real-time experimental application is presented, where a MAS consisting of four rotorcraft UAS successfully performed the tasks of autonomously approaching and escorting a leader, even in the situation when the network topology was arbitrarily changing. Additionally, a Lyapunov stability analysis is included, which demonstrates that the tracking errors between leader and follower agents converge asymptotically to zero. Copyright © 2016 John Wiley & Sons, Ltd.

Received 29 March 2016; Accepted 18 September 2016

KEY WORDS: multi-agent system; adaptive consensus; switching network topology; asset detection and tracking

1. INTRODUCTION

Teams of autonomous vehicles have been proposed to solve a number of problems [1, 2]. Notable among them are environmental monitoring, crop spraying, law enforcement, surveillance and target tracking [3], structural inspection [4–6], mapping [7], as well as search and rescue in disaster response [8, 9].

The main reasons to utilize multiple agents in these scenarios are the robustness of the overall system to failures in individual agents and their ability to operate simultaneously in different regions of the space, which makes the execution of more complex tasks possible. However, endowing these systems with the intelligence necessary to realize the earlier tasks is challenging because, during operation, agents may have access only to limited information such as local perception data or neighboring agents' data that is exchanged using unforeseeable communication links. Deficient exchange of information makes the computation of efficient and reliable solutions intractable, therefore, novel solutions to distributed control and estimation problems that have the potential to reduce the impact of these issues in multi-agent systems (MAS) applications are needed.

*Correspondence to: Hung M. La, Department of Computer Science and Engineering, University of Nevada Reno, NV 89557-0171, USA.
†E-mail: hla@unr.edu

Diverse efforts have been placed on the development of distributed coordination strategies. In general, MAS consensus methodologies [10] are the basis behind these strategies because they enable autonomous formation [11, 12], flocking [13, 14] rendezvous [15, 16] and position synchronization [17].

In a realistic scenario, the agents in a MAS are not homogeneous. For example, in a cooperative MAS team, it could be that a *sensing agent* performs the measurements, and sends its data to a *data processing agent*, which will perform estimation tasks and will possibly transmit an actuation command back to the *sensing agent*. Therefore, an effective communication is essential in the overall performance of the team. In general, a communication link between any two agents can be established when they explicitly exchange information by means of wireless communication links. In addition to enabling sharing data between agents, these links make possible, for example, RF-based agent detection and identification by means of teams of dynamic sensors [18]. On the other hand, an autonomous agent using on-board sensors (imaging, proximity or RF sensors) for estimating the position of a neighboring agent or target is also establishing an implicit unidirectional communication link among them [3]. Unfortunately, unreliable wireless channels and heavy computational loads may affect every kind of communication link and degrade the MAS performance.

Some of the issues introduced by unreliable wireless transmission and their impact on estimation and control have been studied in [19, 20]. Promising solutions for overcoming network issues have been presented in [21, 22]; however, the studied scenarios considered static-agents exclusively. Most of the works on MAS assume ideal communication links, or ideal within a radius and nonexistent outside of it, which cannot be ensured in real-time implementation. The impact of unreliable communication channels on decision-making over a wireless network is still an open research area requiring extensive and realistic studies.

For example, in a real-time disaster response scenario, the robotic agents are expected to be mobile, therefore, the network topology might change over time, which indeed affects the convergence of the consensus. In the worst case, if the network is disconnected (even partially) it is not possible to reach the consensus among agents [23]. There are several recent works which attempted to study the consensus of MAS under a switching topology. In [24], the problem of distributed reliable H_∞ consensus control for high-order MAS was studied. The actuator faults and switching undirected topologies were considered in designing the consensus control. In [25], the consensus reaching of MAS was researched for distributed tracking control problems with general linear agent dynamics and leader's nonzero control input. By using the Markovian chain to model the switching topology, the stochastic consensus problem of linear MAS with communication noises was investigated in [26], in which all agents are assumed to have the same noise-attenuation gain. To relax this assumption, an extension work was proposed in [27]. Particularly, it is possible to deal with topological switching by means of compensation and by treating it as a delta function with impulse actions [28, 29]. Corresponding applications to cooperative multi-robot systems were reported in [30, 31]. An alternative solution to address this issue was reported in [32], where common Lyapunov functions are defined for the average consensus problem with weighting matrix design, for quantized communication on directed switching graphs.

In order to overcome the problems emerging from non-homogeneity and unreliable communication links, this paper proposes adaptive consensus strategies for cooperative MAS subjected to dynamic network topologies and evolving in unfamiliar, unstructured and dynamic environments. Our research is motivated by search and rescue tactics during disaster response, where the detection and tracking of multiple assets (e.g. human beings, chemicals, RF signals and endangered wildlife) is crucial for saving lives and for identifying risk areas.

1.1. Related work

In most of the studies addressing consensus problems, the agents' dynamics are proposed as first-order, second-order or high-order integrators, which can be restrictive in practical situations. One approach to overcome this restriction was presented in [33–35], where authors consider consensus problems in a more general case, using the dynamics of each agent as n-th order linear system. However, in these works the consensus protocols were not implemented in a fully distributed way

DOI: 10.1002/rnc

because of the requirement of knowing the smallest nonzero eigenvalue of the Laplacian matrix, which is a global information that was available to every single agent. Indeed, in a realistic scenario, this information may not widely available, therefore, distributed control laws are crucial for real-time operation of MAS.

In order to overcome this challenge, adaptive consensus protocols have been proposed, where adaptive weights for the communication link between agents were designed, ensuring that consensus is achieved in a fully distributed sense without using global information concerning the communication graph. Among the most promising solutions, authors in [36, 37] and [38] have proposed different methodologies, and their main results and contributions are summarized below:

- In [36] an edge-based adaptive leaderless consensus protocol using only output measurements is addressed without considering the inclusion of a leader, which for many kind of applications that require, for example, to follow a trajectory, could result as a restrictive topology. Additionally, a node-based adaptive leader-follower consensus with a leader of possibly nonzero inputs using only output measurements and the leaderless case under switching topologies were presented. In this work, only simulation results are shown to validate the proposed protocols by using a third order system in the leaderless consensus, and a second order system for the node-based adaptive consensus with a leader of nonzero input.
- In [37], the authors proposed a distributed controller with a node-based adaptive law for updating the coupling gains of a MAS, obtaining simulation results by using second order systems. In this paper, authors used the *sgn* function in the control law in order to improve the robustness of the consensus protocol, which in practical applications could induce the well know chattering effect encountered in Sliding Mode Control methods. Similarly, in this paper all the agents converge to the leader's state, which in practical implementation is not physically possible.
- In [38], the authors developed a distributed relative-state adaptive leaderless consensus, both for the edge-based as well as for the node-based protocols. Additionally, the authors presented a distributed relative-output leaderless adaptive consensus for the node-based protocol. Similarly, in the discontinuous leader-follower adaptive node-based consensus protocol addressed in this related work, authors also considered the *sgn* function, which results in a control law with the chattering effect. In this related work, the authors presented two simulation examples in order to validate the theoretical results they obtained.

Despite being very promising solutions on their own, a unified methodology for addressing and resolving the problems encountered in real-time applications, like the one used as the main motivation of this research paper, is not currently available in the literature. Specifically, a methodology combining an edge-base leader-follower adaptive consensus algorithm under switching topologies has not being previously published. Our work aims at filling this gap by providing meaningful insights concerning the development and the real-time implementation of such a networked MAS, in order to reveal the realistic dynamic behavior and complexity of this kind of systems.

1.2. Preliminary results

The implementation of a MAS in real-life scenarios is a challenging endeavor, which requires an appropriate combination of multiple complementary stages, as well as of several validation steps before obtaining satisfactory results. In this sense, our previous research has presented preliminary efforts to overcome the earlier issues.

In [39], we dealt with the problem of leader-follower MAS tasks by using a linear consensus protocol. This research studied the real-time behavior of the consensus algorithm when applied to the heading and altitude dynamics of a group of four holonomic UAS. On the other hand, our preliminary work [40] presented experimental results on single-agent UAS control strategies enabling the real-time localization and tracking of static and/or dynamic RF sources. A controller for continuous heading rotation was implemented, which allowed rotation of the UAS about its vertical axis, while maintaining a constant altitude hover or a translational displacement. The heading rotation allowed RF bearing estimation by using the received signal strength (RSS) measurements from a directional

DOI: 10.1002/rnc

antenna mounted onboard the UAS, as it avoids the need for additional gimbaling payload. The bearing or Angle of Arrival (AoA) estimate was then utilized by a particle filter for effective source localization and tracking.

Finally, in [41] and [42], we derived approaches for flocking control of a mobile sensor network, aiming at tracking moving targets within changing environments. Additionally, in [43] we presented an adaptive flocking control algorithm for dealing with the problem of flocking control of a mobile sensor network, to track and to observe a moving target in complex environments. A seed growing graph partition (SGGP) algorithm was also proposed to solve the problem of sensor splitting/merging, which allowed to track and to observe multiple targets in a dynamic fashion. In [44], we proposed a distributed sensor fusion scheme based on consensus approach for MAS, aiming at building a scalar field map, while in [45], we presented cooperative and active sensing algorithm for MAS in order to enhance the confidence of the estimate of the scalar field map.

1.3. Main contributions

The main contributions of this paper can be summarized as follows.

- We present an adaptive consensus algorithm which is effective for MAS subjected to switching network topologies. The algorithm guarantees that the team is able to perform escorting tasks (formation and tracking) around the leader (i.e. the asset) position, even in the situation of MAS communication failure, asset detection malfunctioning, the presence of obstacles in the line of sight of some of the agents or uncertain and unexpected issues that cause the MAS to switch to a different communication topology.
- We designed an adaptive leader-follower consensus algorithm based on state feedback, which relaxes the requirement of previously knowing the overall topology of the MAS communication graph. This allow us to implement the consensus algorithm in each agent as a fully distributed consensus protocol, by using a team of multi-rotor aircraft.
- We successfully validated, both in simulations and in real time experiments, the contributions stated earlier. A laboratory experiment was designed which consisted of an asset detection and tracking task, where a team of four holonomic UAS was tasked to detect, to approach and to escort an asset. In this scenario, which is inspired by search and rescue tactics during disaster response, the asset represents a missing person, a RF source, a toxic plume, etc.

Table I summarizes the man differences between some of the related works currently available in the literature and the research findings presented in our manuscript.

The remaining of the paper is organized as follows. In Section 2, we define preliminary concepts and we introduce the MAS mathematical model. Section 3 presents the main contribution of this paper, which are the derived consensus algorithms for MAS under switching network topologies. Section 4 describes a real-life scenario were a MAS may be used for applications related to asset detection and tracking, as in a disaster response event. Next, Section 5 provides the results obtained from both numerical simulations and experimental tests. Finally, Section 6 presents some conclusions, as well as current and future research directions.

Table I. Comparison between our research efforts and the existing literature.

	[36]	[37]	[38]	Our research.
Edge-based Leader-follower protocol	No	No	No	Yes
Node-based Leader-follower protocol	Yes	Yes	Yes	No
Chattering effect	No	Yes	Yes	No
Switching topologies	Yes	No	No	Yes
Formation flight	No	No	No	Yes
Simulation results (system order)	Yes (3rd)	Yes (2nd)	Yes (3rd)	Yes (9th)
Experimental results	No	No	No	Yes

DOI: 10.1002/rnc

2. PRELIMINARIES

This section presents preliminary concepts related to consensus theory. Additionally, the implemented MAS mathematical model is introduced. These definitions provide the fundamental elements required to formulate our main results in the following section.

2.1. Graph theory

A communication graph is used to describe the information exchange between the agents in the MAS, as well as with the MAS leader. Let $\mathcal{G} = (\mathcal{V}, \mathcal{E})$ be a graph with a set of nodes $\mathcal{V} = \{v_1, \ldots, v_N\}$ representing N agents, and a set of edges $\mathcal{E} \subset \mathcal{V} \times \mathcal{V}$. An edge of $\mathcal{E}$ is denoted by (i, j), representing that agent i and agent j can exchange information between them. The graph is undirected if the edges $t(i, j)$ and (j, i) in $\mathcal{E}$ are considered to be the same, otherwise the graph is directed. The graph $\mathcal{G}$ is called connected if there is a path between every pair of nodes, otherwise it is disconnected.

The set of neighbors of node i is denoted by $N_i = \{j : (i, j) \in \mathcal{E}\}$. We define an augmented graph $\bar{\mathcal{G}} = \left(\bar{\mathcal{V}}, \bar{\mathcal{E}}\right)$ to model the interaction topology between N followers and the leader (labeled as v_0). To show which followers are connected to the leader in $\bar{\mathcal{G}}$, we define a leader adjacency matrix $\mathcal{D} = \text{diag}\{d_1, \ldots, d_N\}$ where

$$d_i = \begin{cases} 1 \text{ if follower } v_i \text{is connected to the leader across the communication link } (v_i, v_0) \\ 0 \text{ otherwise} \end{cases}$$

A new augmented Laplacian matrix $\bar{\mathcal{L}}$ for the graph $\bar{\mathcal{G}}$ is defined as

$$\begin{aligned} \bar{\mathcal{L}}_{ii} &= \sum_{j=1, j\neq i}^{N} a_{ij} + d_i \\ \bar{\mathcal{L}}_{ij} &= -a_{ij} \ \ \forall \ i \neq j \end{aligned} \tag{1}$$

where the terms a_{ij} are the elements of an adjacency matrix $\mathcal{A} = [a_{ij}] \in \mathbb{R}^{N\times N}$, and are defined as:

$$a_{ij} = \begin{cases} 0 \text{ if } i = j \\ 1 \text{ if } (i, j) \in \mathcal{E} \\ 0 \text{ otherwise} \end{cases}$$

To describe the variable interconnection topology, the set of all possible graphs is denoted as $S = \{\bar{\mathcal{G}}_1, \bar{\mathcal{G}}_2, \ldots, \bar{\mathcal{G}}_M\}$ with index set $\mathcal{P} = \{1, 2, \ldots, M\}$. The time dependence of the graphs can be characterized by a piece-wise constant switching signal $\sigma : [0, \infty)$ with switching times $t_0, t_1 \ldots$, which represents the index of the topology at time t. Denote by $\bar{\mathcal{G}}_{\sigma(t)}$ the interaction graph between leader and followers, and $\bar{\mathcal{L}}_{\sigma(t)}$ the corresponding augmented Laplacian matrix at time t.

Assumption 1
The undirected graph $\bar{\mathcal{G}}$ is connected.

Lemma 1 ([46]*)*
The matrix $\bar{\mathcal{L}}$ satisfies the following: (i) $\bar{\mathcal{L}}$ has nonnegative eigenvalues, and (ii) $\bar{\mathcal{L}}$ is positive definite if and only if the graph $\bar{\mathcal{L}}$ is connected.

2.2. Mathematical model of the multi-agent system

Consider a MAS consisting of N agents and one leader. In order to represent the agents' translational dynamics in the (X, Y) plane as well as their heading angle (ψ), the dynamics of the i-th agent can be described as

$$\begin{aligned} \dot{x}_i &= Ax_i + Bu_i, \\ y_i &= Cx_i, \quad i = 1, \ldots, N \end{aligned} \tag{2}$$

DOI: 10.1002/rnc

where $x_i \in \mathbb{R}^n$ is the state vector of agent $i, u_i \in \mathbb{R}^p$ is the corresponding control input vector, $y_i \in \mathbb{R}^q$ is the agent's measurement output vector, and A, B and C are constant matrices with compatible dimensions. The dynamics of the leader, labeled as $i = 0$, are given as

$$\dot{x}_0 = Ax_0 \tag{3}$$

where $x_0 \in \mathbb{R}^n$ is the state of the leader.

Assumption 2 (The pair (A, B) is stabilizable)
Because the pair (A, B) is stabilizable, there exists a solution $P > 0$ to the following Algebraic Riccati Equation (ARE)

$$A^T P + PA + Q - PBR^{-1}B^T P = 0 \tag{4}$$

Definition 1
The leader-following consensus problem with a desired formation of the MAS represented by Equations (2)–(3) is said to be solved if for each agent $i \in \{1, \ldots, N\}$, there is a local state feedback u_i such that the closed-loop system satisfies

$$\lim_{t\to\infty} \|(x_i(t) - h_i) - x_0(t)\| = 0 \tag{5}$$

for any initial condition $x_i(0)$, with $i = 0, 1, \ldots, N$, where $h_i \in \mathbb{R}^n$ represents a formation vector $[h_{X,i} \;\; h_{Y,i} \;\; h_{\psi,i}]^\top$ for each agent, associated with a position in the X axis, a position in the Y axis, and a heading angle ψ, respectively.

3. DISTRIBUTED CONSENSUS ALGORITHMS FOR MAS UNDER SWITCHING NETWORK TOPOLOGIES

On its own, consensus algorithms do not allow the implementation of distributed control laws, because they require of previous knowledge of the overall topology of the MAS communication graph. Additionally, consensus algorithms are based on the assumption that the communication graph is fixed. Despite this, due to unexpected situations (MAS communication failure, malfunctioning of sensors for asset detection, the presence of obstacles in the line of sight of some of the agents, etc.) this assumption is hard to fulfill. For this reason, it is crucial to provide the MAS with a network topology switching algorithm that overcomes such scenarios.

This section presents our main result, which are stated as a couple of theorems that allow to deal with the challenges described earlier.

3.1. Adaptive leader-follower consensus

In order for followers track the leader while achieving a desired formation, a distributed formation adaptive control law for each one of the follower agents is designed as follows

$$\begin{aligned} u_i &= K\left(\sum_{j=1}^{N} c_{ij}a_{ij}\left((x_i - h_i) - (x_j - h_j)\right) + c_{i0}d_i\left((x_i - h_i) - x_0\right)\right) \\ \dot{c}_{i0} &= \gamma_{i0}\left((x_i - h_i) - x_0\right)^T \Gamma\left((x_i - h_i) - x_0\right) \\ \dot{c}_{ij} &= \gamma_{ij}a_{ij}\left((x_i - h_i) - (x_j - h_j)\right)^T \Gamma\left((x_i - h_i) - (x_j - h_j)\right) \end{aligned} \tag{6}$$

where $K \in \mathbb{R}^{p\times n}$ and $\Gamma \in \mathbb{R}^{n\times n}$ are feedback matrices to be designed, a_{ij} represents the (i, j)-th entry of the adjacency matrix, and d_i is the (i, i)-th entry of the leader's communication matrix. The time-varying coupling weights of the (i, j) edges are represented by $c_{ij}(t)$, γ_{i0} and $\gamma_{ij} = \gamma_{ji}$, which are positive constants. The following Theorem summarizes our first result, which deals with the problem of distributed consensus.

DOI: 10.1002/rnc

Theorem 1
Consider the MAS described by Equations (2)–(3). Suppose that *Assumption 1* and *Assumption 2* are satisfied. Then, under the consensus protocol defined in Equation (6), with $K = -R^{-1}B^T P$ and $\Gamma = PBR^{-1}B^T P$, where P is the solution of the ARE in Equation (4), all the agents follow the leader from any initial conditions while keeping a predefined formation.

Proof
Let the consensus error be defined as $\delta_i = (x_i - h_i) - x_0$. Then, the consensus error dynamics are given by

$$\begin{aligned} \dot{\delta}_i &= A\delta_i + BK\left(\sum_{j=1}^{N} c_{ij}a_{ij}(\delta_i - \delta_j) + c_{i0}d_i\delta_i\right) \\ \dot{c}_{i0} &= \gamma_{i0}\delta_i^T\Gamma\delta_i \\ \dot{c}_{ij} &= a_{ij}(\delta_i - \delta_j)^T\Gamma(\delta_i - \delta_j) \end{aligned} \tag{7}$$

From Equation (7), it follows that $\delta_i = 0$ if and only if $x_i - h_i = x_0$, with $i = 1, \ldots, N$. Therefore, the consensus problem under the protocol (6) can be reduced to the asymptotic stability of δ_i.

Consider the Lyapunov candidate function

$$V = \sum_{i=1}^{N}\delta_i^T P\delta_i + \sum_{i=1}^{N}\sum_{j=1,j\neq i}^{N}\frac{(c_{ij}-\beta)^2}{2\gamma_{ij}} + \sum_{i=1}^{N}\frac{(c_{i0}-\beta)^2}{\gamma_{i0}} \tag{8}$$

with $0 < P = P^T \in \mathbb{R}^{n\times n}$. The temporal derivative of (8) along the trajectories of system's error (7) is

$$\begin{aligned} \dot{V} = {} & 2\sum_{i=1}^{N}\delta_i^T PA\delta_i + 2\sum_{i=1}^{N}\sum_{j=1}^{N}c_{ij}a_{ij}\delta_i^T PBK(\delta_i - \delta_j) + 2\sum_{i=1}^{N}c_{i0}d_i\delta_i^T PBK\delta_i \\ & + \sum_{i=1}^{N}\sum_{j=1,j\neq i}^{N}\frac{(c_{ij}-\beta)}{2}\left(a_{ij}(\delta_i - \delta_j)^T\Gamma\left(\delta_i - \delta_j\right)\right) + \sum_{i=1}^{N}(c_{i0}-\beta)(d_i\delta_i^T\Gamma\delta_i) \end{aligned} \tag{9}$$

Because the graph is undirected, the following is obtained

$$\sum_{i=1}^{N}\sum_{j=1,j\neq i}^{N}(c_{ij}-\beta)a_{ij}(\delta_i - \delta_j)^T\Gamma(\delta_i - \delta_j) = 2\sum_{i=1}^{N}\sum_{j=1}^{N}(c_{ij}-\beta)a_{ij}\delta_i^T\Gamma(\delta_i - \delta_j) \tag{10}$$

Substituting $K = -R^{-1}B^T P, \Gamma = PBR^{-1}B^T P$, and Equation (10) into Equation (9) we obtain

$$\dot{V} = 2\sum_{i=1}^{N}\delta_i^T PA\delta_i - 2\beta\sum_{i=1}^{N}\sum_{j=1}^{N}a_{ij}\delta_i^T PBR^{-1}B^T P(\delta_i - \delta_j) - 2\beta\sum_{i=1}^{N}d_i\delta_i^T PBR^{-1}B^T P\delta_i \tag{11}$$

From the leader-follower topology matrix $\bar{\mathcal{L}} = \mathcal{L} + \mathcal{D}$ we have

$$\begin{aligned} & -2\beta\left(\sum_{i=1}^{N}\sum_{j=1}^{N}a_{ij}\delta_i^T PBR^{-1}B^T P(\delta_i - \delta_j) + \sum_{i=1}^{N}d_i\delta_i^T PBR^{-1}B^T P\delta_i\right) \\ & = -2\beta\sum_{i=1}^{N}\sum_{j=1}^{N}\bar{\mathcal{L}}_{ij}\delta_i^T PBR^{-1}B^T P\delta_j \end{aligned} \tag{12}$$

Rewriting $\dot{V}$ as

$$\dot{V} = \sum_{i=1}^{N}\delta_i(A^T P + PA)\delta_i - 2\beta\sum_{i=1}^{N}\sum_{j=1}^{N}\bar{\mathcal{L}}_{ij}\delta_i^T PBR^{-1}B^T P\delta_j \tag{13}$$

DOI: 10.1002/rnc

and defining an error consensus vector $\delta = \left[\delta_1^T, \ldots, \delta_N^T\right]^T$, a compact form expression for $\dot{V}$ can be written as

$$\dot{V} = \delta^T \left(I_N \otimes (A^T P + PA) - 2\beta \bar{\mathcal{L}} \otimes PBR^{-1}B^T P\right)\delta \tag{14}$$

From *Lemma 1* and *Assumption 1*, the matrix $\bar{\mathcal{L}}$ satisfies $\bar{\mathcal{L}} = \bar{\mathcal{L}}^T > 0$. Therefore, there exists an orthogonal matrix $T \in \mathbb{R}^{N\times N}$ such that

$$T\bar{\mathcal{L}}T^T = \Lambda := \text{diag}(\lambda_1, \ldots, \lambda_N) \tag{15}$$

where $\lambda_1, \ldots, \lambda_N$ are the matrix $\bar{\mathcal{L}}$ eigenvalues, which are positives. Consider the transformation $\tilde{\delta} = (T \otimes I_n)\,\delta$, then, the Lyapunov temporal derivative in Equation (22) is rewritten as

$$\begin{aligned}\dot{V} &= \tilde{\delta}^T \left(I_N \otimes (A^T P + PA) - \Lambda \otimes (PBR^{-1}B^T P)\right)\tilde{\delta} \\ &= \sum_{i=1}^{N} \tilde{\delta}_i^T \left(A^T P + PA + Q - 2\beta\lambda_i PBR^{-1}B^T P\right)\tilde{\delta}_i - \sum_{i=1}^{N} \tilde{\delta}_i^T Q \tilde{\delta}_i\end{aligned} \tag{16}$$

with $0 < Q = Q^T \in \mathbb{R}^{n\times n}$. By choosing β sufficiently large in such a way that $2\beta\lambda_i \geqslant 1$ is fulfilled for all $i = 1, \ldots, N$, it follows that

$$A^T P + PA + Q - 2\beta\lambda_1 PBR^{-1}B^T P \leqslant A^T P + PA + Q - PBR^{-1}B^T P \tag{17}$$

Then, the following is obtained

$$\dot{V} \leqslant \sum_{i=1}^{N} \tilde{\delta}_i^T \left(A^T P + PA + Q - PBR^{-1}B^T P\right)\tilde{\delta}_i - \sum_{i=1}^{N} \tilde{\delta}_i^T Q \tilde{\delta}_i \tag{18}$$

If *Assumption 2* holds, then, there exists a solution $P > 0$ for the following control ARE

$$A^T P + PA + Q - PBR^{-1}B^T P = 0 \tag{19}$$

Therefore,

$$\dot{V} = -\sum_{i=1}^{N} \tilde{\delta}_i^T Q \tilde{\delta}_i \leqslant 0 \tag{20}$$

Because $\dot{V} \leqslant 0$, then $V(t)$ is bounded and so is each c_{ij}, which converges to some finite value because $\Gamma \geqslant 0$. Note that $\dot{V}_1 = 0$ implies that $\delta_i = 0$ for the N agents. Therefore, by LaSalle's invariance principle, it follows that the consensus error $\delta(t) \to 0$ as $t \to \infty$, solving the problem of distributed consensus. □

3.2. Extension to switching topology

In order to guarantee that the MAS is able to perform escorting flight (formation and tracking) around the leader position, even in the situation of unexpected issues affecting the MAS connectivity between agents, we propose an adaptive consensus algorithm for MAS subjected to switching topologies. The following Theorem summarizes our second result.

Theorem 2
Assume that *Assumption 1* and *Assumption 2* hold. For arbitrary switching communication graphs $\bar{\mathcal{G}}_{\sigma(t)}$ belonging to set S, the MAS described by Equations (2)–(3) under the consensus protocol (6) with $K = -R^{-1}B^T P$ and $\Gamma = PBR^{-1}B^T P$, where P is the solution of ARE in (4), ensures the follower agents follow the leader agent from any initial conditions, while keeping a predefined formation.

DOI: 10.1002/rnc

Proof
Consider the switching event as an 'arbitrary switching' providing the MAS with a switching network topology that allows effective performance under different scenarios. A necessary and sufficient condition for a switching system to be asymptotically stable under arbitrary switching is the existence of a common Lyapunov function [47]. Considering a common Lyapunov function

$$V = \sum_{i=1}^{N} \delta_i^T P \delta_i + \sum_{i=1}^{N} \sum_{j=1, j\neq i}^{N} \frac{\left(c_{ij} - \beta\right)^2}{4\gamma_{ij}} + \sum_{i=1}^{N} \frac{(c_{i0} - \beta)^2}{2\gamma_{i0}} \tag{21}$$

Using the definitions and procedures exposed in *Theorem 1*, we obtain the time derivative of V along the trajectory of the error dynamics (7) as

$$\begin{aligned} \dot{V} &= \delta^T \left(I_N \otimes (A^T P + PA) - 2\beta \bar{\mathcal{L}}_\sigma(t) \otimes PBR^{-1}B^T P\right) \delta \\ \dot{V} &= \sum_{i=1}^{N} \tilde{\delta}_i^T \left(A^T P + PA + Q - 2\beta\lambda_i PBR^{-1}B^T P\right) \tilde{\delta}_i - \sum_{i=1}^{N} \tilde{\delta}_i^T Q \tilde{\delta}_i \end{aligned} \tag{22}$$

For each $p \in \mathcal{P}$, define $\tau_p := \rho(\bar{\mathcal{L}})$ as the smallest nonzero eigenvalue of $\bar{\mathcal{L}}$. Because $\mathcal{P}$ is finite, the set $\{\tau_p \ : \ p \in \mathcal{P}\}$ is finite. Define

$$\tau_{\min} := \min\{\tau_p : p \in \mathcal{P}\} \tag{23}$$

which is positive and independent of time. With the definition of $\tau_{\min}$, the following is obtained for $\dot{V}$

$$\dot{V} = \sum_{i=1}^{N} \tilde{\delta}_i^T \left(A^T P + PA + Q - 2\beta\tau_{\min} PBR^{-1}B^T P\right) \tilde{\delta}_i - \sum_{i=1}^{N} \tilde{\delta}_i^T Q \tilde{\delta}_i \tag{24}$$

Similar to *Theorem 1*, by choosing β sufficiently large such that $2\beta\delta_{\min} \geqslant 1$ is satisfied, and because $\bar{\mathcal{G}}_{\sigma(t)}$ is connected, we obtain

$$\dot{V}(t) = \tilde{\delta}_i^T Q \tilde{\delta}_i \leqslant 0 \tag{25}$$

Using similar arguments than those applied in *Theorem 1*, by LaSalle's invariance principle it is shown that the consensus error $\delta(t) \to 0$ as $t \to \infty$. Therefore, the Equation (21) is a common Lyapunov function for the MAS represented by (2)–(3). Then, asymptotic stability under arbitrary switching topology is achieved. □

4. APPLICATION: DEVELOPMENT OF A MAS FOR ASSET DETECTION AND TRACKING

This section describes a real world scenario, where the proposed distributed consensus algorithms for MAS affected by switching network topologies may be useful. The application chosen in our study takes inspiration from the idea of using a team of unmanned systems for accomplishing the task of asset detection and tracking. This scenario could happen for example, when a team of robots is tasked to find a missing person after a natural disaster, or when it is desired to find the location of a toxic plume by means of autonomous agents. Location of endangered wildlife, RF sources and heat sources, among others, are also among the list of possible applications.

In this work, we adopted *search* and *approach* strategies for autonomous asset detection and tracking, which are inspired by the chemotactical motion of the bacterium E. coli [48, 49]. Interestingly, this bacterium is unable to perceive chemical spatial gradients, however, it is still able to follow the gradient of a chemical attractant, despite the rotational diffusion that constantly changes the bacterium orientation. The E. coli accomplishes the gradient following by switching between two alternate behaviors: *run* and *tumble*. In the run phase, the E. coli swims with constant velocity by rotating its flagella in the counter-clockwise direction. In the tumble phase, by rotating its flagella in the clockwise direction, the bacterium spins around without changing its position. The less improvement the bacterium senses in the concentration of the attractant during the run phase, the

DOI: 10.1002/rnc

more probable a direction change (tumble) becomes [48]. This motion leads to a distribution whose peak coincides with the maximum of the sensed quantity.

In order to accomplish the asset detection, each autonomous agent must be equipped with an appropriate sensor suit, which may vary among the different members of the MAS, and must be selected according to the mission to be accomplished. For example, for the situation when the agents must locate an RF source (e.g. when a wild animal carrying a bracelet has to be found) the sensor suit must contain a compass and a directional antenna, which are capable of providing a direction or bearing angle at which the RF source (i.e. the animal or asset) can be found. This is where the E. coli *tumble* behavior is used: the autonomous agent is tasked to rotate around its own axis without changing its position. Indeed, this motion in combination with the onboard sensors data will lead to a distribution whose peak coincides with the bearing angle at which the maximum of the sensed RF signal is found.

In addition to the onboard sensor suit, each agent must carry a communication device. With this system, each agent will be able to share, with all of its neighbors, its own location as well as the bearing angle measurement pointing towards the asset. Once this information has been shared, each agent can use its own data and the received data to execute a triangulation procedure, whose output will be a (possible planar) coordinate at which the asset can be found. The communication network is also needed for implementing the distributed consensus algorithm that will enable the MAS to operate as a coordinated cooperative team. To this end, the source location coordinate will be used as a *leader agent* which must be approached and followed by the robots in the MAS. This is similar to the E. coli *run* behavior previously explained.

Once the MAS has reached the radiation source's position, the agents must perform an escorting task (formation and tracking) around it, in order to provide real-time data of the object of interest. To guarantee a successful execution of the mission, keeping an effective escorting is crucial. Therefore, the escorting task must be ensured even in the situation when the MAS communication is subjected to failures, the sensors for asset detection are not working properly, or when the presence of obstacles in the line of sight of some of the agents prevent an appropriate observation of the asset, among others.

Aiming at reducing the complexity of a real-time implementation, the overall objective of asset detection and tracking by means of a MAS has been separated in five complementary stages (or modules).

4.1. Module 1: Communication. Establishing a communication protocol for the agents in the MAS

The first task to be accomplished deals with establishing the communication protocol between neighboring agents. Figure 1 depicts the communication scheme that we implemented in order to enable the transmission and reception of the information needed by each agent. The main purpose of the mesh is to share information between agents, which depends on the employed consensus topology. To this end, we propose a wireless network based on a mesh topology that enables each agent to send and receive Micro Air Vehicle Communication Protocol (MAVLink) messages by using API commands. This kind of protocol allows to easily include additional agents to the MAS, as well as to integrate the MAS to another network based on the same protocol. Furthermore, compatibility with other projects, software or autopilots is guaranteed, which allows us to create a fully scalable sensor network.

4.2. Module 2: Estimation. Determining the direction at which the asset is located

In this stage, each agent makes use of its onboard sensors to estimate a bearing angle associated with the direction at which the asset is located. A control strategy is implemented for this specific stage, which allows the agent to rotate several times about its own z-axis (vertical axis) until the sensing device determines a bearing angle at which the source can be encountered, for example, the bearing angle at which the received signal strength of an RF source or the concentration of a chemical exhibits a maximum value [40]. Figure 2 illustrates the agents' behavior during this stage. Notice also the estimated bearing angle resulting from this procedure, which is, so far, the best individual approximation of the asset's location.

DOI: 10.1002/rnc

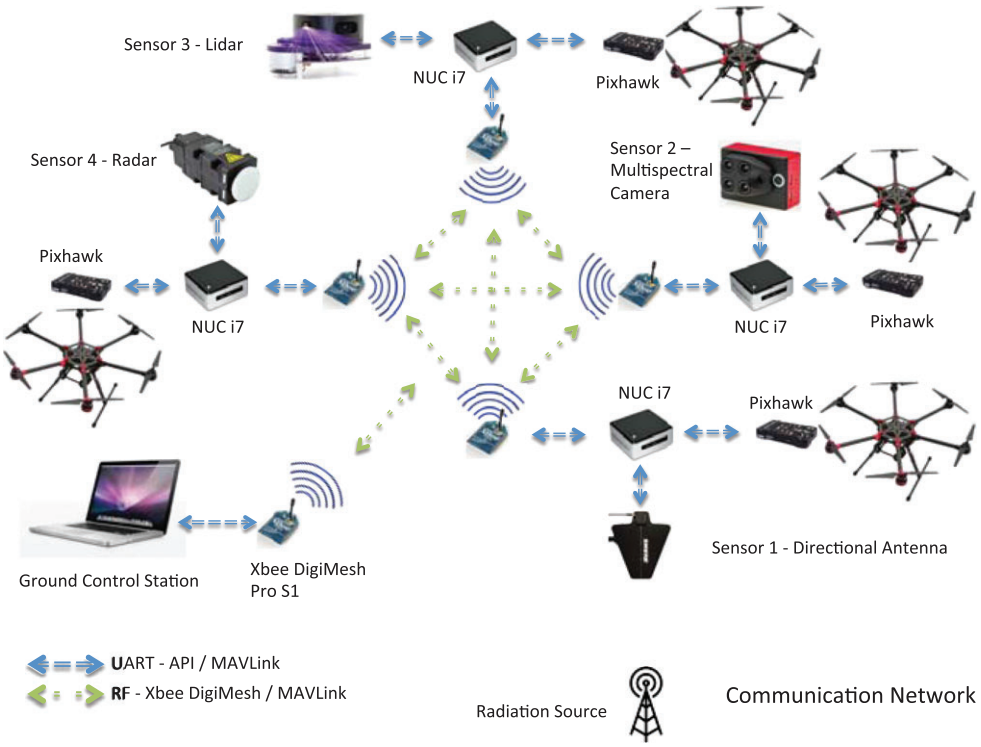

Figure 1. The proposed communication network enables the transmission and reception of the information needed by each agent. The Figure shows an example of the hardware involved in the communication network, which is formed by set of components onboard each agent in the MAS and can involve: asset detection sensors (Lidar, Radar, Directional antennas, Multi spectral cameras, chemical detector, heat detector, etc.) which are selected according to the mission to be executed, RF modems for sending/receiving data, onboard computer for networking data processing, and autopilot computers. A ground control station is also included in the MAS, which may act as a static agents capable of performing intensive computations.

4.3. Module 3: Triangulation. Obtaining an estimate of the asset coordinates

Once every agent (or in some situations, until some of them) has locally obtained an estimate describing the bearing angle at which the asset can be found, each agent transmits such information as well as its own coordinates to all of its neighbors. This procedure will enable to obtain, by means of combining all the available measurements in a triangulation procedure, an accurate estimate of the asset location in planar coordinates. The algorithm combining the estimated bearing angles of the neighbor agents is based on the implementation of an Extended Kalman Filter. Figure 3 shows the triangulation points that each agent can determine based on the employed network topology.

4.4. Module 4: Approaching the source. Implementation of the adaptive consensus algorithm to reach the asset

This stage makes use of the asset's coordinates in the (X, Y) plane, in combination with an adaptive consensus algorithm for collectively stabilizing the forward, lateral and heading dynamics of each agent around the location of the asset. In the proposed approach, the coordinates of the asset will be used as the coordinates of a *leader agent* for the MAS team. The proposed controller allows the MAS to move towards and to reach the asset (leader), and also to perform escorting behaviors if needed (e.g. if the asset is dynamic). Figure 4 depicts an example of specific trajectories that the agents in the MAS have performed in order to coordinate and to reach, as an organized team, the asset (leader) location. Notice that, in order to avoid collisions between agents, a flocking controller is needed.

DOI: 10.1002/rnc

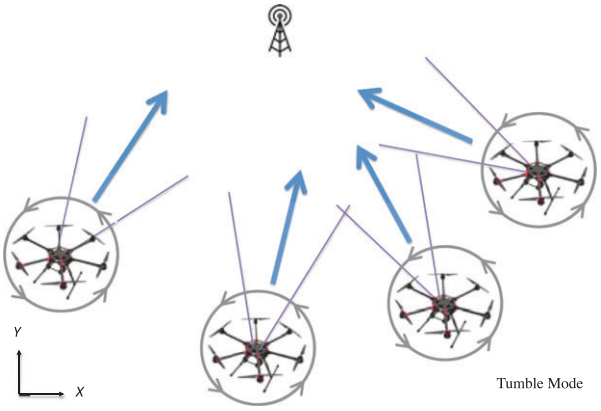

Figure 2. Tumble Mode. In this mode, each agent rotates multiple times around its z-axis until its onboard sensors provide a directional measurement associated with the bearing angle at which the asset can be found.

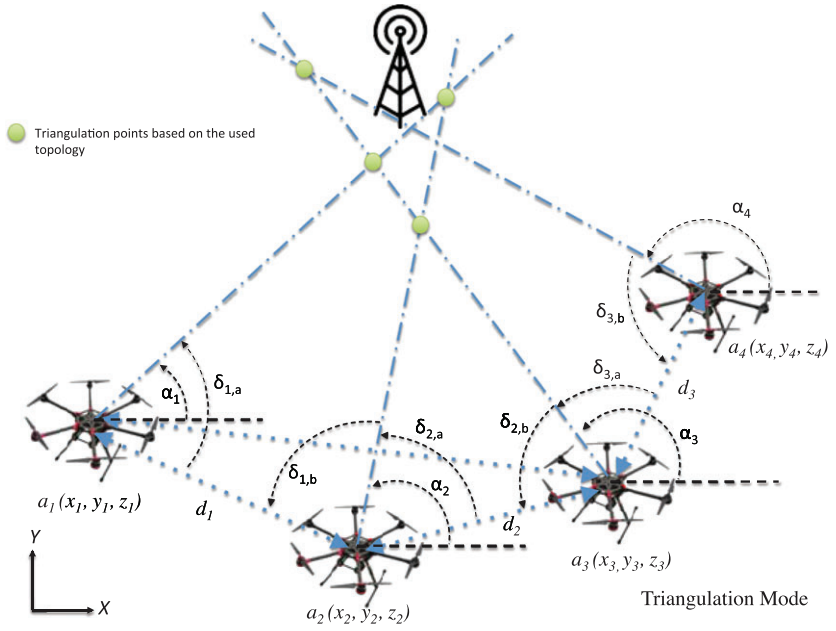

Figure 3. The source triangulation is obtained by means of combining the measurements and location of each agent with the (similar) information received from its neighbors.

4.5. Module 5: Escorting. Tracking and observing the asset or source

The last stage is devoted to maintaining the MAS in an escorting flight behavior around the asset (i.e. the formation leader). This procedure is based on the implementation of a switching adaptive consensus algorithm, which is crucial for enabling real-time operations. While performing the escorting task, each agent is tasked to maintain a specific heading angle towards the asset, as well as specific coordinates in the (X, Y) plane, determined by the location the leader plus a previously defined offset to ensure a specific formation. The proposed approach will allow proper functioning of the MAS during the entire mission, even in the scenario of a possible loss of communication, a failure in some of the asset detection sensors, the presence of an obstacle in the line of sight of the agents, noise in the wireless network or some other issue that causes the links of the network to be dynamic. Notice that all of these undesired issues will trigger switching to a different network topology. Figure 5 shows the formation flight and escorting behavior once the team of agents has

DOI: 10.1002/rnc

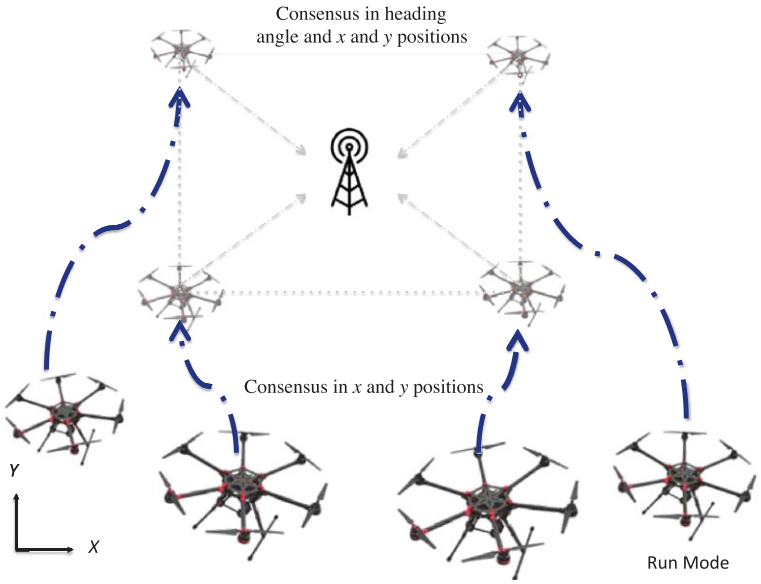

Figure 4. In this stage, each agent flies towards the asset location, taking into account its neighbors' coordinates, and attracted by the adaptive coupling weight c_{ij} implicit in the communication graph.

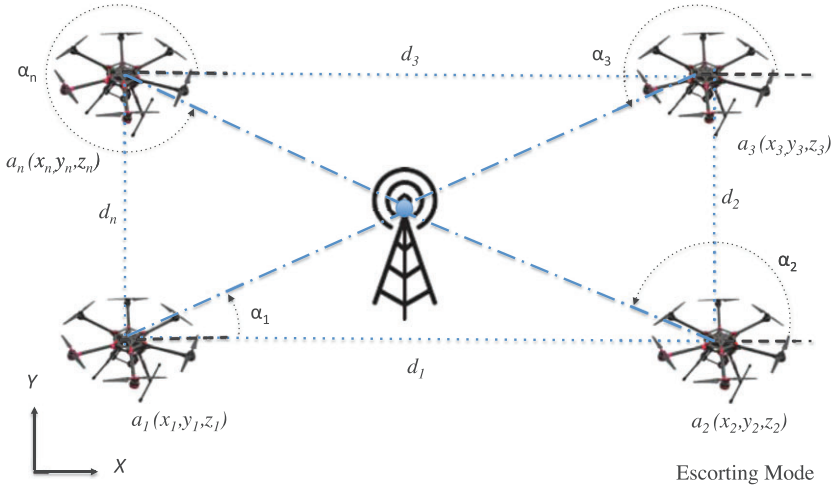

Figure 5. Escorting Mode. In this mode, the MAS is able to perform an escorting flight around the source, which may be static or dynamic. Furthermore, the proposed strategy allows the MAS to maintain a proper functionality under uncertain environments.

reached the asset. The proposed algorithm makes possible to execute tracking tasks in the situation of having a dynamic source, or in the situation of evolving under dynamic environments.

5. SIMULATION AND EXPERIMENTAL RESULTS

In order to validate the performance of the MAS control strategies by means of numerical simulations as well as of real time experiments, it is necessary to obtain a mathematical model describing the dynamics of each agent in the system.

At this point, it is worth mentioning that most of the commercially available UAS platforms are equipped with onboard computers which deal with the stabilization of the vehicle's angular dynamics, that is, they run an inner control loop for attitude stabilization (hover). Additionally, the inner control loop is programmed to accept external control inputs influencing the translational

DOI: 10.1002/rnc

dynamics of the UAS. This characteristic allows a human pilot to take control of the 3-dimensional motion of the UAS by means of control commands, which are commonly generated by a joystick or a cellphone, and are sent to the UAS by means of wifi or RF signals.

Because of this characteristic, we focus our attention on the dynamics and controllers that will affect the UAS heading angle and displacement in the (X, Y) plane (outer control loop), and we left the inner control loop to take care of the attitude stabilization of the vehicle. This controller's subdivision is also valid from the point of view of the decoupling of the aerial vehicle's dynamics, see for example [50] and [51].

Towards this end, we used a modeling procedure which is based on the step response methodology, and whose detailed description can be found in our previous work [39]. The dynamic models obtained correspond to the translational dynamics in the (X, Y) axes, as well as the heading angle (ψ) of a quad rotorcraft UAS. Specifically, the models are

(i) *Dynamic model for heading angle* (ψ)

$$\dot{x}_{\psi,i} = \begin{bmatrix} 0 & 1 & 0 \\ 0 & 0 & 1 \\ 0 & -156.25 & -10.25 \end{bmatrix} x_{\psi,i} + \begin{bmatrix} 0 \\ 0 \\ 15625 \end{bmatrix} u_{\psi,i} \tag{26}$$

(ii) *Dynamic model for translation in the* X *axis*

$$\dot{x}_{X,i} = \begin{bmatrix} 0 & 1 & 0 \\ 0 & 0 & 1 \\ 0 & -1.21 & -2.42 \end{bmatrix} x_{X,i} + \begin{bmatrix} 0 \\ 0 \\ 9922 \end{bmatrix} u_{X,i} \tag{27}$$

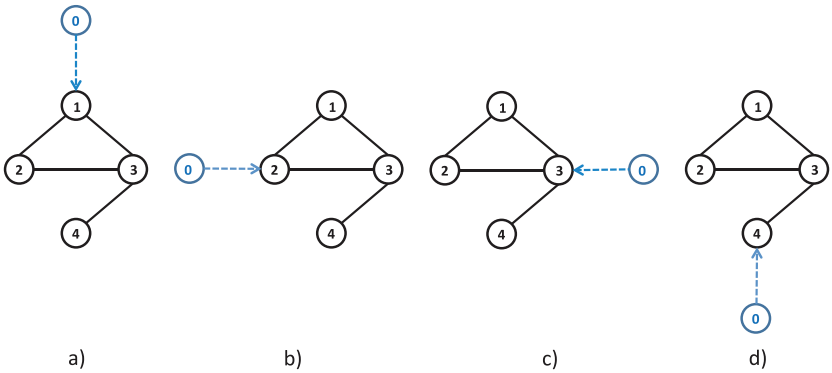

Figure 6. Leader Switching Topology: the follower MAS agents, labeled $\{1, 2, 3, 4\}$, maintain a fixed network topology. On the other hand, four different network topology scenarios are considered, which arise from switching the leader 'connection' with the rest of the agents in the MAS.

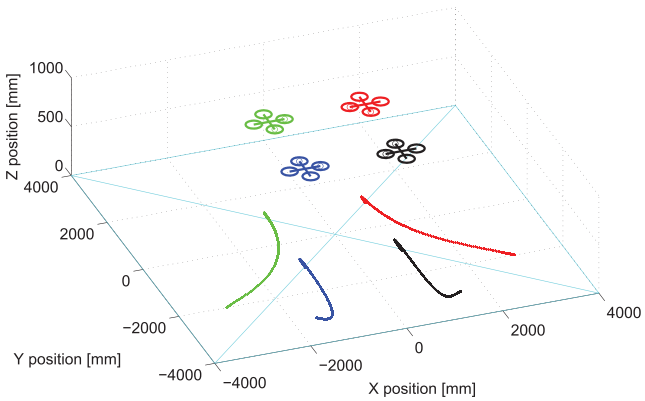

Figure 7. A 3-dimensional simulation result showing the overall sketch of the mission to be performed.

DOI: 10.1002/rnc

(iii) *Dynamic model for translation in Y axis*

$$\dot{x}_{Y,i} = \begin{bmatrix} 0 & 1 & 0 \\ 0 & 0 & 1 \\ 0 & -1.21 & -2.64 \end{bmatrix} x_{Y,i} + \begin{bmatrix} 0 \\ 0 \\ 9801 \end{bmatrix} u_{Y,i} \tag{28}$$

The consensus protocol in Equation (6) requires the gains K and Γ. By solving the ARE in (4), the gains are obtained as follows

(i) *Gains for heading angle*

$$K_\psi = -\begin{bmatrix} 0.0258 & 0.0020 & 0.0002 \end{bmatrix}, \quad \Gamma_\psi = \begin{bmatrix} 1.0000 & 0.0791 & 0.0083 \\ 0.0791 & 0.0063 & 0.0007 \\ 0.0083 & 0.0007 & 0.0001 \end{bmatrix} \tag{29}$$

(ii) *Gains for translation in X*

$$K_X = -\begin{bmatrix} 0.0015 & 0.0014 & 0.0003 \end{bmatrix}, \quad \Gamma_X = \begin{bmatrix} 0.2800 & 0.2571 & 0.0638 \\ 0.2571 & 0.2360 & 0.0586 \\ 0.0638 & 0.0586 & 0.0145 \end{bmatrix} \tag{30}$$

(iii) *Gains for translation in Y*

$$K_Y = -\begin{bmatrix} 0.0015 & 0.0014 & 0.0003 \end{bmatrix}, \quad \Gamma_Y = \begin{bmatrix} 0.2800 & 0.2598 & 0.0621 \\ 0.2598 & 0.2410 & 0.0577 \\ 0.0621 & 0.0577 & 0.0138 \end{bmatrix} \tag{31}$$

In this work, it is considered that the follower MAS agents, labeled $\{1, 2, 3, 4\}$, maintain a fixed network topology. On the other hand, four different network topology scenarios are considered, which arise from switching the leader 'connection' with the rest of the agents in the MAS. The switching topologies are presented in Figure 6.

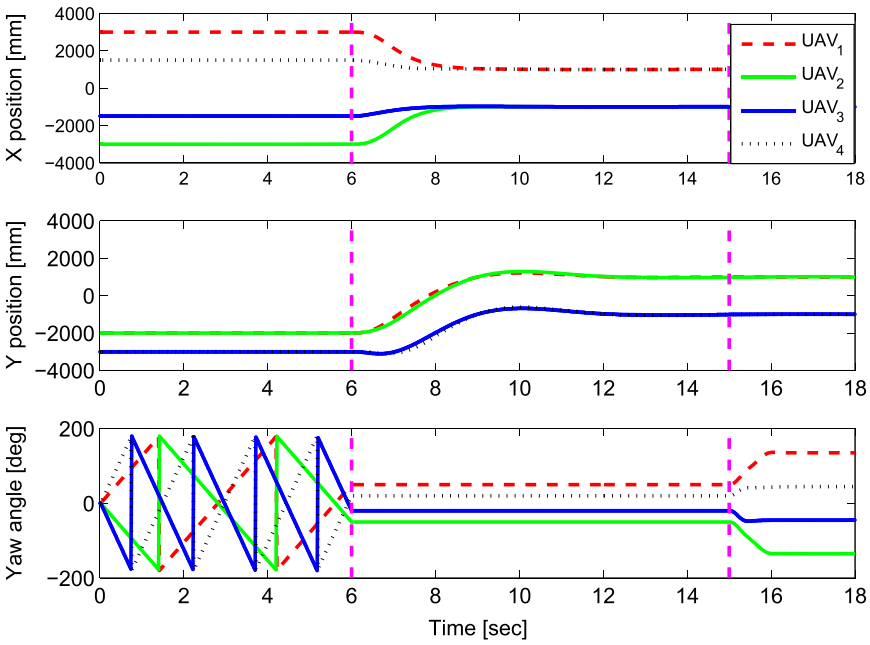

Figure 8. Simulation results: During the first stage, the MAS robots rotate around its z-axis, at different speed rates, emulating the *tumble mode*. Here, each agent is obtaining a measurement associated with a bearing angle at which the asset can be found. After 6 s, the adaptive consensus algorithm is executed, and the MAS starts approaching to the asset or source. Finally, once the source is located at the center of the MAS, the adaptive consensus algorithm for switching network topologies is executed, This happens after 15 s of operation. This algorithm is crucial in this stage because it ensures that each agent is able to perform the escorting flight around the asset, even when the detection or 'communication' with the leader is unreliable.

DOI: 10.1002/rnc

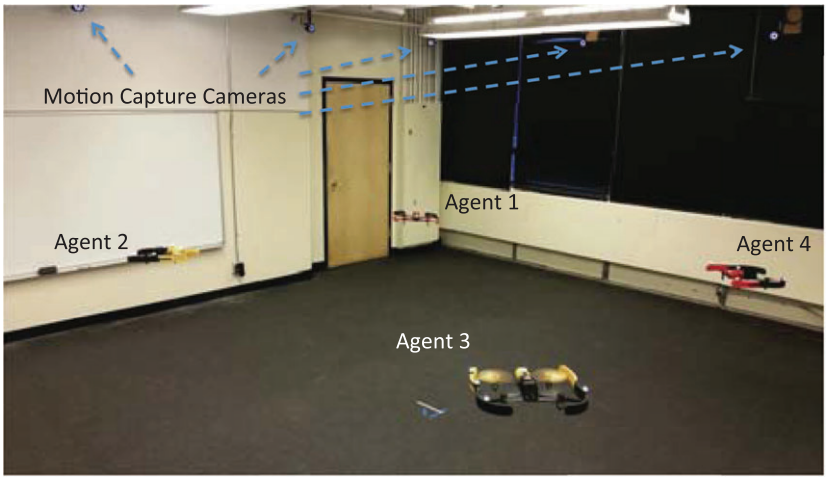

Figure 9. Experimental Platform consisting of four Bebop Drones, a motion capture system, and a ground station computer executing ROS. The image shows the Drones while performing the approaching task. Some of the motion capture system cameras can be seen fixed to the wall.

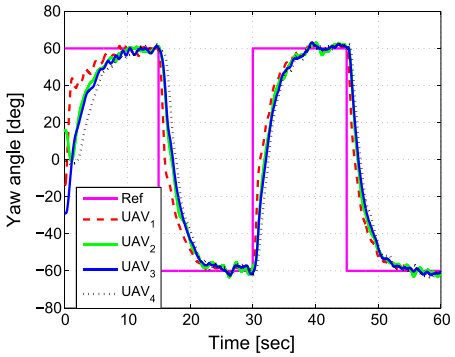

(a) Adaptive consensus in heading dynamics

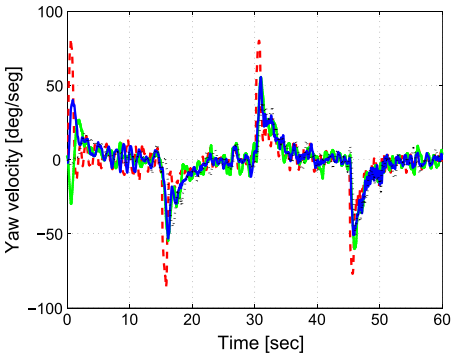

(b) Velocity consensus in heading dynamics.

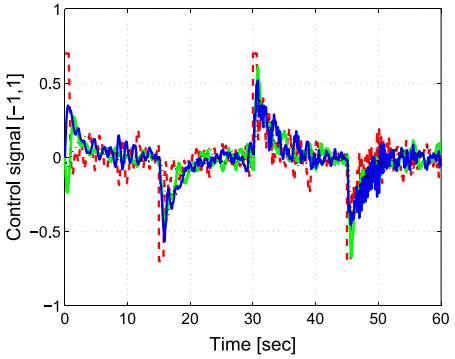

(c) Control signals for stabilization of heading dynamics

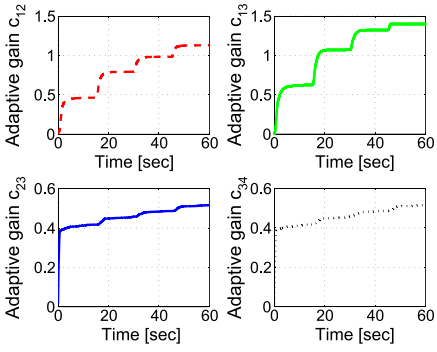

(d) Adaptive gains for stabilization of heading dynamics.

Figure 10. Adaptive consensus in heading dynamics.

DOI: 10.1002/rnc

5.1. *Simulation results*

To validate the proposed MAS distributed control laws, a set of numerical simulations is presented, which represent the asset detection and tracking application, and consist of the following modules: (i) the stage when each agent in the MAS is rotating around its Z-axis, (ii) the stage when the agents are approaching to the radiation source, and (iii) the stage when the MAS team is performing the escorting flight around the asset (i.e. MAS leader) with an offset of 90° in the heading angle of each agent.

Figures 7 and 8 show the translational and heading dynamics of each agent, for the situation when they start the mission at random initial states. During the first stage, each agent rotates around its z-axis, at different speed rates, emulating the **tumble mode** in which each agent is estimating an initial measurement of a bearing angle towards the asset. After 6 s in this mode, the adaptive consensus algorithm is executed. Then, the MAS starts approaching the source, and the agents reach a formation around it. Finally, after 15 s of operation, the adaptive consensus algorithm for switching network topologies is executed. This algorithm is crucial in this stage because it ensures that each agent is able to perform the escorting flight around the asset, even when the detection or 'communication' with the leader is unreliable.

5.2. *Experimental results*

We now proceed with the implementation of the proposed distributed consensus strategies considering switching network topologies in a real-time application: asset detection and tracking by means of a team of four rotorcraft UAS. The following assumptions are made with the main objective of focusing our efforts in the approaching and escorting stages previously described.

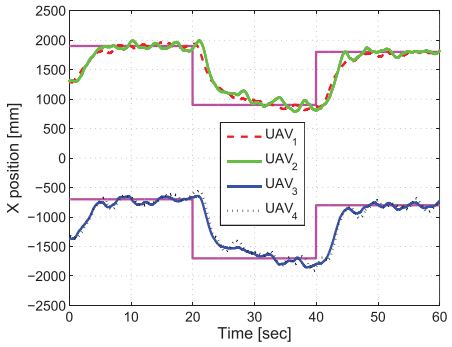

(a) Adaptive Consensus in X-axis dynamics

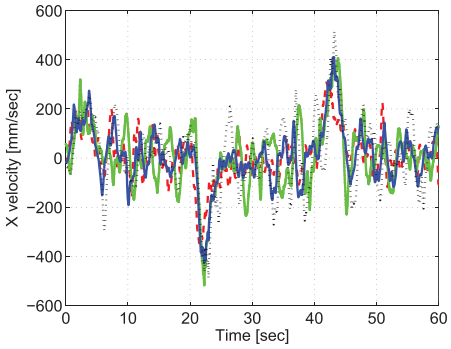

(b) Adaptive Consensus in X-axis velocity dynamics

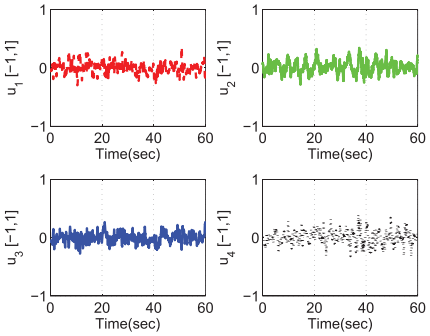

(c) Control signals for stabilization of X-axis dynamics

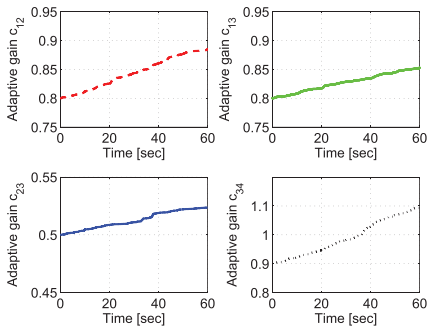

(d) Adaptive gains for stabilization of X-axis dynamics

Figure 11. Adaptive consensus in X-axis dynamics.

DOI: 10.1002/rnc

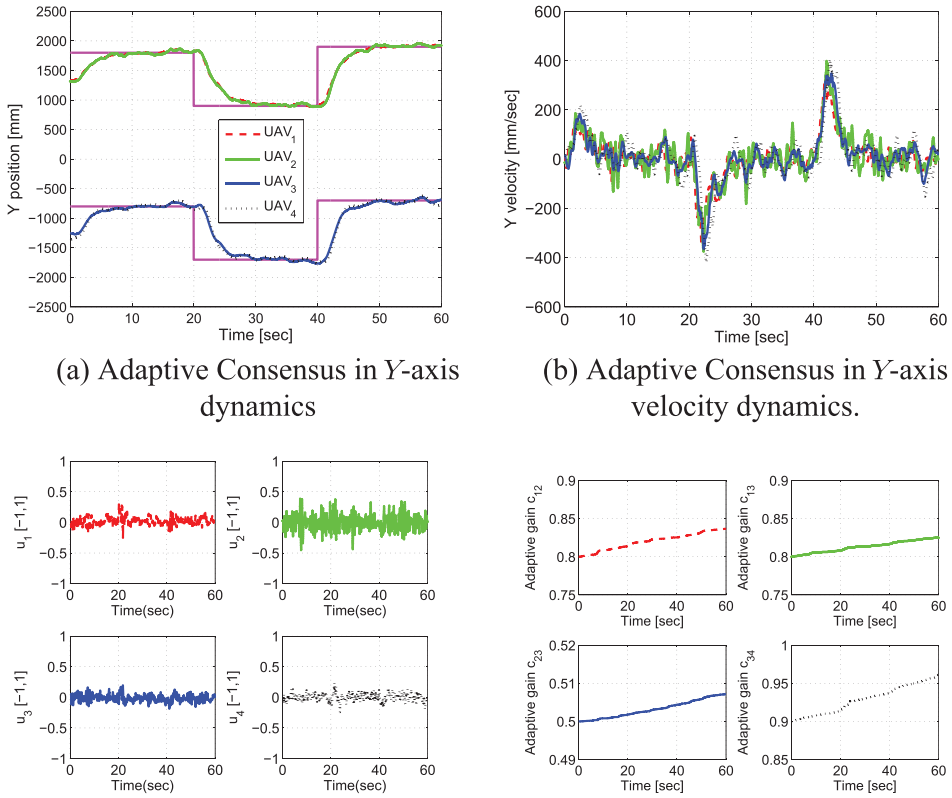

(a) Adaptive Consensus in Y-axis dynamics

(b) Adaptive Consensus in Y-axis velocity dynamics.

(c) Control signals for stabilization of Y-axis dynamics

(d) Adaptive gains for stabilization of Y-axis dynamics

Figure 12. Adaptive consensus in Y-axis dynamics.

(1) The MAS agents are able to obtain a bearing measurement associated with the asset/source location. This is possible due to an embedded sensor (which may vary according to the agent/mission characteristics).
(2) The MAS agents are able to communicate with its neighbors, at least sporadically.
(3) By using the bearing angle towards the source, in combination with a robust triangulation procedure, the planar coordinates of the asset are accurately obtained.
(4) The MAS agents are able to perform flocking flight in order to avoid collisions between them during operation.

Taking into account these previous assumptions, we implemented an experimental setup consisting of four Bebop Drones developed by Parrot, an OptiTrack motion capture system consisting of twelve Prime 13 cameras, and a computer running Robot Operating System (ROS) libraries and tools, which communicates every 20 ms with the drones by means of WiFi. The motion capture system was used in order to obtain the ground truth (translational and angular coordinates) of each agent in the MAS. The asset (or leader of the formation) was implemented as a virtual entity. Figure 9 shows the Bebop drones flying during the approaching mode. Some of the cameras of the motion capture system can also be seen at the top of the image.

In order to test the developed consensus protocols, a set of preliminary experiments was executed. These tests allowed us to validate, individually, the performance of each one of the dynamics to be controlled, that is, motion along the X axis, motion along the Y axis, and heading angle. In these experiments, the MAS followed a reference square signal. The results obtained are shown in Figures 10–13, where it can be observed the agents position, velocity, control signals, as well as the adaptive gains obtained for each one of the experiment.

DOI: 10.1002/rnc

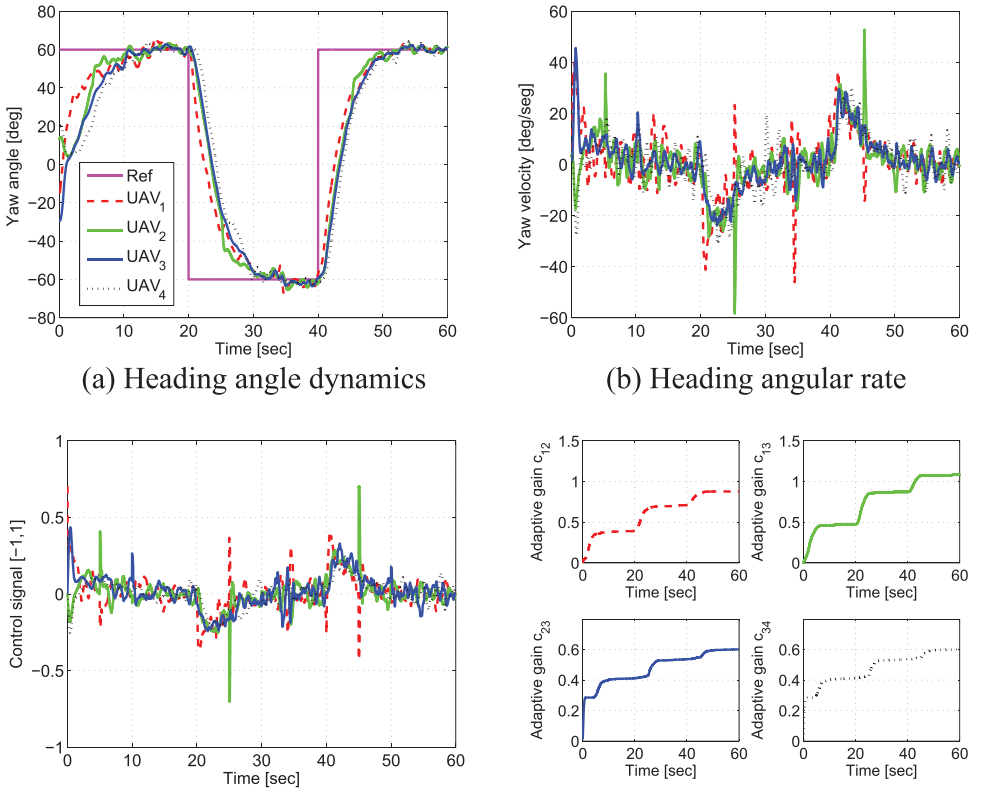

(a) Heading angle dynamics

(b) Heading angular rate

(c) Control input for heading angle stabilization

(d) Adaptive gains for heading angle stabilization

Figure 13. Adaptive consensus under switching network topologies: heading dynamics.

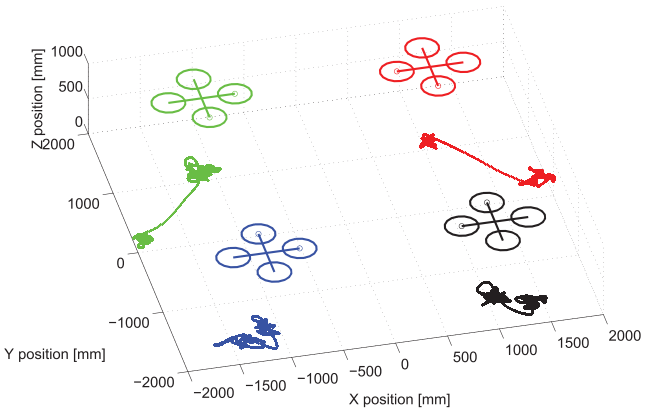

Figure 14. Real-time experiments: a 3-dimensinal plot showing the evolution of the agents' states during the execution of the following modules: (i) tumble mode, (ii) approaching mode and (iii) escorting mode. The asset or source (which represents the MAS leader) is implemented as a virtual entity located at the (0,0) planar coordinate. The translational behavior of each agent is projected in the (X, Y) plane for illustration purposes. Notice how the agents states are stabilized in coordinates representing the corners of a square around the asset.

DOI: 10.1002/rnc

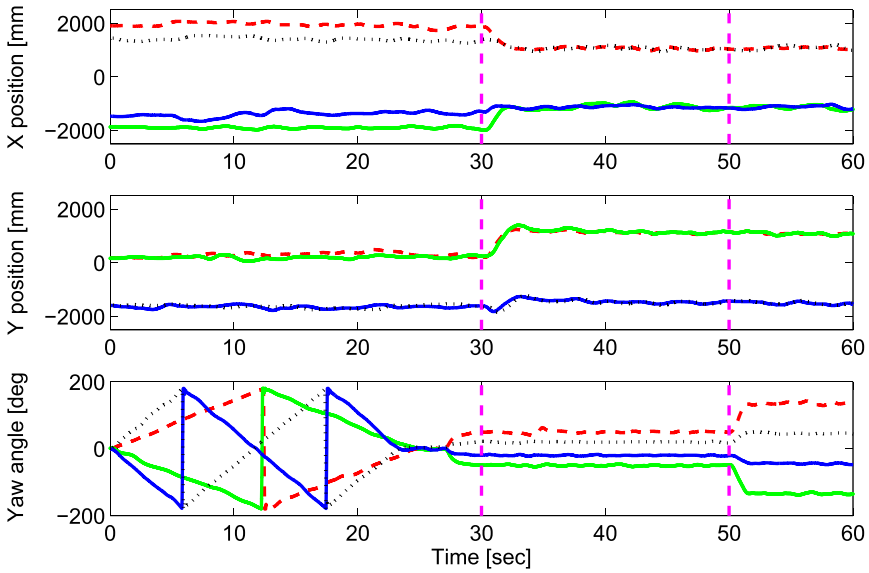

Figure 15. Real-time experiments: the plots show the evolution of the agents' states during the execution of the following modules: (i) tumble mode, (ii) approaching mode and (iii) escorting mode. The upper graphic shows the translation of the agents in the X-axis. The central plot shows the translation of the agents in the Y-axis. From these previous plots, notice how the agents states are stabilized in coordinates representing the corners of a square around the asset. The lower graphic shows the heading dynamics of the agents during the test. Notice that, during the tumble mode, the agents rotate, at different speeds, around its vertical axis. Next, during the approaching mode the heading angles are kept at constant values. Finally, when the MAS team is performing the escorting flight around the asset (i.e. MAS leader) the heading dynamics are stabilized in such a way each agent is pointing towards the source location. Because the final formation is a square, an offset of 90° between agents is obtained.

Figure 10(a)–(d) shows the performance of the adaptive consensus protocol applied to the heading angle dynamics (ψ) of the MAS robots (Bebop rotorcrafts). Additionally, the set of Figure 11(a)–(d) shows the performance of the adaptive consensus protocol applied to the stabilization of the X-translational dynamics of the agents. Finally, Figure 12(a)–(d) shows the performance of the adaptive consensus protocol applied to the stabilization of the Y-translational dynamics of agents.

Figure 13(a)–(d) shows the performance of the adaptive consensus protocol for MAS stabilization performing under switching network topologies. The strategy is applied to the stabilization of the heading angle dynamics of the MAS rotorcrafts. In order to include the effects of network malfunction, a network topology switching is applied every 5 s, between the four topologies presented in Figure 6. The switching sequence applied corresponds to $\{1, 2, 3, 4, 1, 2, 3, 4, \ldots\}$. In Figure 13(b)–(c) it can be observed the effect of the network switching. Specifically, when a network switching occurs, the control signals and the velocity dynamics exhibit small increments.

Finally, Figures 14 and 15 show the results obtained from the experimental test of the following modules: (i) tumble mode, (ii) approaching mode and (iii) escorting mode. Notice that, in this experiment, the agents' behavior is similar to the behavior obtained in the numerical simulations.

A video showing both the simulation and the experimental results previously described can be found at https://youtu.be/Y8Pdzf0oz2Y

6. CONCLUSIONS

A distributed adaptive consensus algorithm for stabilization of a MAS affected by switching network events was proposed and implemented. Because the coupling gain of the associated graph is adapted dynamically in real-time, each agent in the MAS is able to compute its own control law based on its own information and the information from its neighbors. Under this approach, it is not necessary to have access to global information ensuring a fully distributed operation. The switching network

DOI: 10.1002/rnc

topology strategy was designed and included in the distributed consensus algorithm in order to address the situation when a change in the MAS network topology is needed. For real-time MAS operations, a change in the MAS network topology may occur due to undesired issues such as a failure in the communication network, a sensor failing to provide a measurement of the asset, the presence of obstacles in the line of sight of the agents, etc.

Our main results were stated as a couple of theorems, and stability proofs were provided. Simulation results were also presented in order to validate the performance of the proposed methodologies. As an ultimate test, we designed an implemented a real-time experiment consisting of the tasks of: (i) approaching an asset, and (ii) escorting the asset, by means of a MAS. To this end, an experimental test-bed consisting of a MAS composed by four quad rotorcraft UAS platforms, in combination with a motion capture system, was used. The MAS successfully performed the autonomous approaching and the escorting of the asset, even in the situation when the network topology was changing. These results are the first steps towards a full real-time implementation of the overall asset location goal described in Section 4.

Current and Future Research Directions

Current directions of our work explore stopping rules allowing the agents to decide when an appropriate bearing angle towards the source has been obtained. Furthermore, we are currently exploring the inclusion of nonlinear terms in the mathematical model of each agent, which will allow us to derive a control law to deal with nonlinear phenomenons implicit in the system. Another research direction will explore a flocking control law including a collision avoidance term between agents, while performing the asset detection and tracking task. Finally, the performance of external experiments by using a wireless network is also envisioned in order to validate the effectiveness of our methodology in a realistic non-controlled environment.

ACKNOWLEDGEMENTS

This work was partially supported by the Nevada Advanced Autonomous Systems Innovation Center, by the Mexican Secretariat of Public Education (SEP) grant PRODEP UPPACH-004, by the Project *Red Temática de Sistemas Autónomos y Ciber-Físicos*, and by the Mexican National Council for Science and Technology grant 263777.

REFERENCES

1. Erdmann M, Lozano-Perezm T. On multiple moving objects. *Algorithmica* 1987; **2**(1):477–521.
2. Belta C, Kumar V. Abstraction and control for groups of robots. *IEEE Transactions on Robotics* 2004; **20**(5):865–875.
3. Garcia Carrillo LR, Russell WJ, Hespanha JP, Collins GE. State estimation of multi-agent systems under impulsive noise and disturbances. *IEEE Transactions on Control Systems Technology* 2015; **23**(1):13–26.
4. Bircher A, Kamel M, Alexis K, Burri M, Oettershagen P, Omari S, Mantel T, Siegwart R. Three-dimensional coverage path planning via viewpoint resampling and tour optimization for aerial robots. *Autonomous Robots* 2016; **40**(6):1059–1078.
5. Alexis K, Papachristos C, Siegwart R, Tzes A. Uniform Coverage Structural Inspection Path-Planning for Micro Aerial Vehicles. *IEEE Multiconference on Systems and Control*, Sydney NSW, 2015; 59–64.
6. Bircher A, Alexis K, Burri M, Oettershagen P, Omari S, Mantel T, Siegwart R. Structural inspection path planning via iterative viewpoint resampling with application to aerial robotics. *IEEE International Conference on Robotics and Automation (ICRA)*, Seattle, WA, 6423.
7. Oettershagen P, Stastny T, Mantel T, Melzer A, Rudin K, Agamennoni G, Alexis K, Siegwart R. Long-endurance sensing and mapping using a hand-launchable solar-powered UAV. Field and Service Robotics (FSR), 2016; 441–454. Volume 113 of the series Springer Tracts in Advanced Robotics.
8. Agcayazi MT, Cawi E, Jurgenson A, Ghassemi P, Cook G. ResQuad: Toward a semi-autonomous wilderness search and rescue unmanned aerial system. *2016 International Conference on Unmanned Aircraft Systems (ICUAS)*, Arlington, VA, 2016; 898–904.
9. Papachristos C, Tzoumanikas D, Alexis K, Tzes A. Autonomous Robotic Aerial Tracking, Avoidance, and Seeking of a Mobile Human Subject. *Advances in Visual Computing* 2015; **9474**(1):444–454.
10. Vamvoudakis KG, Garcia Carrillo LR, Hespanha JP. Learning consensus in adversarial environments. *Proceedings of the SPIE-8741 Defense, Security and Sensing, Unmanned Systems Technology*, Baltimore, Maryland, 2013; 1–8.
11. Fax JA, Murray RM. Information flow and cooperative control of vehicle formations. *IEEE Transactions on Automatic Control* 2004; **49**:1465–1476.

DOI: 10.1002/rnc

12. Glavaski S, Chaves M, Day R, Nag P, Williams A, Zhang W. Vehicle networks: Achieving regular formation. *American Control Conference*, 2003; 4095–4100.
13. Tanner HG, Jadbabaie A, Pappas GJ. Stable flocking of mobile agents, Part I: Fixed topology. *IEEE Conference on Decision and Control*, Maui, HI, 2003; 2010–2015.
14. Tanner HG, Jadbabaie A, Pappas GJ. Stable flocking of mobile agents, Part II: Dynamic topology. *IEEE Conference on Decision and Control*, Maui, HI, 2003; 2016–2021.
15. Lin J, Morse AS, Anderson BDO. The multi-agent rendezvous problem. *IEEE Conference on Decision and Control*, Maui, Hi, 2003; 1508–1513.
16. Alexis K, Nikolakopoulos G, Tzes A, Dritsas L. Coordination of helicopter UAVs for aerial forest-fire surveillance, 2009; 169–193.
17. Rodriguez-Angeles A. Cooperative synchronization of robots via estimated state feedback. *IEEE Conference on Decision and Control*, Maui, Hi, 2003; 1514–1519.
18. Paik JK. Image processing-based mine detection techniques using multiple sensors: A review. Subsurface Sensing Technologies and Applications. *An International Journal* 2002; **3**:203–252.
19. Wong W, Brockett R. Systems with finite communication bandwidth constraints - Part I: State estimation problems. *IEEE Transactions on Automatic Control* 1997; **42**(9):1294–1299.
20. Faganini F, Zampieri S. Stability analysis and synthesis for scalar linear systems with a quantized feedback. *IEEE Transactions on Automatic Control* 2003; **48**(9):1569–1584.
21. Liu X, Goldsmith AJ. Cross-layer design of distributed control over wireless networks. *Advances in Control, Communication Networks, and Transportation Systems:In Honor of Pravin Varaiya*, Systems & Control:Foundations & Applications (Series), Birkhäuser Boston, MA, 2005; 111–136.
22. Feng-Li L, Moyne J, Tilbury D. Network design consideration for distributed control systems. *IEEE Transactions on Control Systems Technology* 2002; **10**(2):297–307.
23. Olfati-Saber R, Fax JA, Murray RM. Consensus and cooperation in networked multi-agent systems. *Proceedings of the IEEE* 2007; **95**(1):215–233.
24. Wang X, Yang GH. Distributed reliable H_∞ consensus control for a class of multi-agent systems under switching networks: A topology-based average dwell time approach. *International Journal of Robust and Nonlinear Control* 2016; **26**(13): 2767–2787.
25. Li Z, Liu X, Ren W, Xie L. Distributed tracking control for linear multiagent systems with a leader of bounded unknown input. *IEEE Transactions on Automatic Control* 2013; **58**(2):518–523.
26. Wang Y, Cheng L, Ren W, Hou ZG, Tan M. Seeking consensus in networks of linear agents: Communication noises and markovian switching topologies. *IEEE Transactions on Automatic Control* 2015; **60**(5):1374–1379.
27. Cheng L, Wang Y, Ren W, Hou ZG, Tan M. On convergence rate of leader-following consensus of linear multi-agent systems with communication noises. *IEEE Transactions on Automatic Control* 2016; **PP**(99):1–6.
28. Li S, Guo Y. Distributed consensus filter on directed graphs with switching topologies, 2013; 6151–6156.
29. Li S, Guo Y. Distributed consensus filter on directed switching graphs. *International Journal of Robust and Nonlinear Control* 2015; **25**(13): 2019–2040.
30. Li S, Kong R, Guo Y. Cooperative distributed source seeking by multiple robots: Algorithms and experiments. *IEEE/ASME Transactions on Mechatronics* 2014; **19**(6):1810–1820.
31. Li S, Guo Y, Bingham B. Multi-robot cooperative control for monitoring and tracking dynamic plumes. *IEEE International Conference on Robotics and Automation (ICRA)*, Hong Kong, 2014; 67–73.
32. Li S, Guo Y, Fang J, Li H. Average consensus with weighting matrix design for quantized communication on directed switching graphs. *International Journal of Adaptive Control and Signal Process* 2013; **27**(6):519–540.
33. Zhongkui L, Zhinsheng D, Guangrong C, Lin-Huang. Consensus of multiagent systems and synchronization of complex networks: A unified viewpoint. *IEEE Transactions on Circuits and Systems* 2010; **57**(1):213–224.
34. Jin S, Hyungbo S, Juhoon B. Consensus of high-order linear systems using dynamic output feedback compensator: Low gain approach. *Automatica* 2009; **45**:2659–2664.
35. Hongwei Z, Frank L, Abhijit D. Optimal design for synchronization of cooperative systems: State feedback, observer and output feedback. *IEEE Transactions on Automatic Control* 2011; **56**(8):1948–1952.
36. Li Z, Ren W, Liu X, Xie L. Distributed consensus of linear multi-agent systems with adaptive dynamic protocols. *Automatica* 2013; **49**:1986–1995.
37. Li Z, Ren W, Liu X, Fu M. Consensus of Multi-Agent systems with general linear and Lipschitz nonlinear dynamics using distributed adaptive protocols. *IEEE Transactions on Automatic Control* 2013; **58**(7):1786–1791.
38. Li Z, Duan Z. Distributed consensus protocol design for general linear multi-agent systems: a consensus region approach. *IET Control Theory and Applications* 2014; **8**(18):2145–2161.
39. Ortega G, Mũnoz F, Espinoza Quesada ES, Garcia Carrillo LR, Ordaz P. Implementation of leader-follower linear consensus algorithm for coordination of multiple aircrafts. *3rd Workshop on Research, Education and Development of Unmanned Aerial Systems*, Cancun, Mexico, 2015; 25–32.
40. Isaacs JT, Quitin F, Garcia Carrillo, Madhow U, Hespanha JP. Quadrotor control for rf source localization and tracking. *The 2014 International Conference on Unmanned Aircraft Systems*, Orlando, FL, 2014; 244–252.
41. La HM, Sheng W. Adaptive flocking control for dynamic target tracking in mobile sensor networks. *The 2009 IEEE/RSJ International Conference on Intelligent Robots and Systems*, St. Louis, MO, 2009; 4843–4848.
42. La HM, Sheng W. Flocking control of a mobile sensor network to track and observe a moving target. *IEEE International Conference on Robotics and Automation Kobe International Conference Center*, Kobe, Japan, 2009; 3129–3134.

DOI: 10.1002/rnc

43. La HM, Sheng W. Dynamic target tracking and observing in a mobile sensor network. *Robotics and Autonomous Systems* 2012; **60**(7):996–1009.
44. La HM, Sheng W. Distributed sensor fusion for scalar field mapping using mobile sensor networks. *IEEE Transactions on Cybernetics* 2013; **43**(2):766–778.
45. La HM, Sheng W, Chen J. Cooperative and active sensing in mobile sensor networks for scalar field mapping. *IEEE Transactions on Systems, Man and Cybernetics: Systems* 2015; **45**(1):1–12.
46. Ni W, Cheng D. Leader-following consensus of multi-agent systems under fixed and switching topologies. *System & Control Letters* 2010; **59**:209–217.
47. Zhao J, Hill DJ. On stability, L2-gain and H∞ control for switched systems. *Automatica* 2008; **44**(5):1220–1232.
48. Berg H, Brown D. Chemotaxis in Escherichia coli analyzed by three-dimensional tracking. *Nature* 1972; **239**(5374):500–504.
49. Alt W. Biased random walk models for chemotaxis and related diffusion approximations. *Journal of Mathematical Biology* 1980; **9**(2):147–177.
50. Garcia Carrillo LR, Espinoza ES, Mondie S. Controller's parameters tuning in presence of time-delay measurements: an application to vision-based quad-rotor navigation. *51st IEEE Conference on Decision and Control*, Maui, Hawaii, 2012; 5667–5672.
51. Ramirez A, Espinoza ES, Garcia Carrillo LR, Mondie S, Garcia A, Lozano R. Stability analysis of a vision-based UAV controller: An application to autonomous road following missions. *Journal of Intelligent and Robotic Systems* 2014; **74**(1):69–84.

DOI: 10.1002/rnc